

ORIGINAL ARTICLE

Sex-specific analysis of microRNA profiles in HBV-associated cirrhosis by small RNA-sequencing

Kristy Kwan-Shuen Chan¹ | Kwan-Yung Au¹ | Wai-Ching Fung¹ |
Cheuk-Yan Wong¹ | Albert Chi-Yan Chan^{2,3} | Regina Cheuk-Lam Lo^{1,3} 

¹Department of Pathology, School of Clinical Medicine, The University of Hong Kong, Hong Kong, China

²Department of Surgery, School of Clinical Medicine, The University of Hong Kong, Hong Kong, China

³State Key Laboratory of Liver Research (The University of Hong Kong), Hong Kong, China

Correspondence

Regina Cheuk-Lam Lo, Department of Pathology, School of Clinical Medicine, The University of Hong Kong, Queen Mary Hospital, Pokfulam, Hong Kong, China.
Email: reginalo@pathology.hku.hk

Funding information

University of Hong Kong; Faculty of Medicine

Abstract

Liver cirrhosis represents an advanced stage of chronic liver disease and is associated with significant morbidity, mortality, and risk of cancer development. While sex disparity of liver diseases has been observed, understanding at a genetic level awaits more thorough investigation. In this study, we performed a sex-specific analysis of the microRNA (miR) profiles in hepatitis B virus (HBV)-associated cirrhosis by small RNA-sequencing using clinical tissue samples. Potential associated signaling pathways, downstream gene targets, and upstream regulators were highlighted by computational prediction analyses based on the differentially expressed miRs (DEmiRs). From our results, deregulation of miRs in cirrhosis showed a marked difference between males and females by the degree and pattern. Sixty-five (64 up-regulated, 1 down-regulated) and 12 (6 up-regulated, 6 down-regulated) DEmiRs were found in males and females, respectively, when compared with their respective control group. A number of DEmiRs were only observed in one sex but not the other. In addition, 26 DEmiRs were identified between cirrhosis female and cirrhosis male groups. Fatty acid biosynthesis pathway, extracellular matrix-receptor interaction, p53 signaling, Hippo signaling, tumor necrosis factor signaling, the forkhead box O signaling, as well as gene targets ribosomal protein S27 like, methyl CpG binding protein 2, and estrogen receptor 1, may contribute to the pathogenesis and biological behavior of cirrhosis in a sex-specific manner. Analysis of the Cancer Genome Atlas data set suggested a role of sex-specific DEmiRs in multistep hepatocarcinogenesis. *Conclusion:* Our findings illustrate that miR profiles in HBV-associated cirrhosis are distinct between the males and females and suggest a potential role of sex-specific biomarkers and molecular mechanisms in disease development and progression.

This is an open access article under the terms of the [Creative Commons Attribution-NonCommercial-NoDerivs](https://creativecommons.org/licenses/by-nc-nd/4.0/) License, which permits use and distribution in any medium, provided the original work is properly cited, the use is non-commercial and no modifications or adaptations are made.

© 2022 The Authors. *Hepatology Communications* published by Wiley Periodicals LLC on behalf of American Association for the Study of Liver Diseases.

INTRODUCTION

Cirrhosis represents an advanced stage of chronic liver disease (CLD) and is a major cause *per se* for liver-related mortality. Chronic hepatitis B (CHB) virus infection is the top-ranking etiology for cirrhosis in Southeast Asia. The annual incidence of CHB to cirrhosis in Asians ranged from 0.1–2.8 per 100 person-years, with a 5-year cumulative incidence of 17%.^[1] The annual incidence of hepatic decompensation and liver-related mortality is 2–4 and 2.9 per 100 person-years in the Asian population, respectively.^[1] In 2016, cirrhosis was one of the most common indications (51%) for liver transplantation in our center.^[2] In addition, cirrhosis is a risk factor for primary liver cancer, with about 80% of hepatocellular carcinoma (HCC) associated with cirrhosis.

Activation of hepatic stellate cells and fibroblasts is a key cellular event during fibrogenesis. Transforming growth factor β (TGF- β)/mothers against decapentaplegic homolog (SMAD) and WNT signaling cascades were implicated in liver fibrogenesis.^[3] At the genomic level, the mutational landscape has been illustrated using clinical samples in a recent report.^[4] In this regard, clues from the clinical and epidemiological perspectives may also provide insights on the dissection of molecular mechanisms in human diseases. Remarkably, sex disparity is characteristically observed in CLD and HCC. For example, autoimmune liver diseases and drug-induced liver injury showed a higher incidence in women than men.^[5] Conversely, disease progression of CHB was more rapid in men.^[6,7] Worse still, the male sex was identified as an independent risk factor for cirrhosis.^[1] Risk of disease-related death was reported to be higher in male than female patients.^[8–10] HCC by itself has a higher incidence in males than females with a 5–7:1 ratio.^[9] Among patients with cirrhosis, females have better outcome than males in terms of HCC incidence and overall survival.^[11] Consistently, the genetic content in hepatitis B virus (HBV)–related HCC was found to be different between the two sexes in terms of copy number variation.^[12] Hence, it is plausible that genetic events in CLD could be sex-specific throughout the multistep process.

These pieces of information made us speculate that while cirrhosis appears similar histologically, the molecular signatures may be different between the sexes. This is an important investigative question, as the divergent biological processes may infer a need for sex-specific monitoring and intervention during the multistep clinical course of CHB infection. Thus far, factors accounting for sex disparity are still poorly understood. Sex hormones were one of the first targets investigated for their contribution to the disparity. Male chronic HBV carriers with a higher androgen level progress to HCC at a faster rate.^[13,14] Because the HBV genome contains androgen responsive elements, androgen signaling

pathway mechanistically promotes hepatocarcinogenesis via inhibition of the tumor suppressor gene.^[15]

In this study, we aimed at unmasking the potential difference in the microRNA (miR) profiles of HBV-associated cirrhosis between males and females. miR is a type of noncoding RNA well known for their epigenetic regulatory functions on gene expression, rendering it a potential useful biomarker. Deregulation of miR was identified from CHB to HCC.^[16–18] Moreover, miRs are therapeutic targets. Use of miR-21 inhibitor was reported to be effective in a preclinical model for fibrotic disease in the heart.^[19] Alteration of miR profiles in HCC was found to correlate with clinical parameters such as etiology and deregulation specific of signaling pathways.^[20] Interestingly, differential miR expression was observed between male and female patients with HCC.^[21] As far as cirrhosis is concerned, an enormous effort was put to analyze serum samples obtained from patients with CHB. With clinical tissue samples, a few studies demonstrated the deregulated expression of isolated or a small panel (up to 17) of miRs, and two studies examined the miR profiles by microarray.^[22,23] Thus far, deep-sequencing data from HBV-cirrhotic liver tissues are scarce, let alone the potential sex disparity in miR profiles is rarely characterized.

Cirrhosis represents a critical tipping point for investigation. Moreover, the growing body of evidence on regression of liver cirrhosis upon antiviral treatment^[24] necessitates a re-examination of the molecular pathogenesis of cirrhosis. Intervention to revert the genetic changes at this stage can also effectively prevent liver-related morbidity and mortality and the development of liver cancer, a deadly cancer despite advances in surgical intervention and targeted therapy. In this study, we carried out miR profiling by small RNA-sequencing (sRNA-seq) using clinical tissue samples from HBV-associated cirrhosis. Our analyses demonstrated that the miR profiles in HBV-associated cirrhosis displayed distinct patterns between males and females, and revealed potential sex-specific biomarkers and molecular mechanisms contributing to fibrogenesis and tumorigenesis.

METHODS

Clinical samples

Formalin-fixed paraffin-embedded (FFPE) clinical tissue samples were retrospectively retrieved from the archive in Department of Pathology, Queen Mary Hospital, Hong Kong. For the test groups, liver explant specimens with a diagnosis of HBV-associated cirrhosis from adult patients were used. Nontumoral liver tissue in liver metastasectomy specimens collected from adult patients with metastatic cancers were used as the control groups. Histological features of the liver

(cirrhosis or normal) were reviewed by a histopathologist (RCL), and images were captured with Nanozoomer S210 (Hamamatsu Photonics). Macrodissection was performed if necessary. Use of clinical samples was approved by the Institutional Review Board of the University of Hong Kong/Hospital Authority Hong Kong West Cluster (HKU/HA HKW IRB; ref: UW 20–696 and UW 12–525).

RNA extraction from FFPE sections and sRNA-seq

Total RNA was extracted from eight 4- μ m FFPE sections per case using the miRNeasy FFPE kit according to the manufacturer's instruction (Qiagen). Deparaffinization was done using xylene followed by graded ethanol wash. RNA was eluted in 20 μ l of RNase-free water and stored at -80°C before use. Quality control of extracted small RNA, library preparation, and sRNA-seq was conducted by the Centre for PanorOmic Sciences, HKU. Quality and quantity of extracted RNA was analyzed by Agilent 2100 bioanalyzer using RNA 6000 Nano total RNA assay (Agilent Technologies) and Qubit 2.0 fluorometer using the RNA HS assay kit (Thermo Fisher Scientific), respectively. Qualified RNA (100 ng) samples were subjected to library preparation, which was done using NEBNext Multiplex Small RNA library Prep Set for Illumina (v6.0; New England Biolabs). The adaptor-ligated libraries were enriched by 15 cycles of polymerase chain reaction (PCR) followed by purification and size selection using BluePippin platform according to manufacturer's protocol (Sage Science). PCR products ranging between 125 bp and 155 bp were subsequently selected for sRNA-seq (2×151 bp) with the Illumina NovaSeq 6000.

Bioinformatics and computational analyses

Sequencing reads were assigned to each sample using bcl2fastq (Illumina). Number of reads, total throughput, and the quality score, as denoted by Q30, were determined for each sample. Sequencing reads were filtered for adapter sequence. Low-quality sequence, defined as reads with more than 5% unknown bases or more than 50% of bases with quality value less than 10, were excluded. Sequencing reads (≥ 15 bp) were retained. Read alignments were performed using Bowtie2 (v2.2.5). Filtered reads were mapped to human mature miR sequence, and unmapped reads were mapped to hairpin miR sequence (miRBase v21). Reads aligned to reference genome were counted using HTSeq-count (v0.6.0) for each gene-biotype. Alignment and read counts were performed using default parameters with following exceptions: length of the seed substrings to

align during multiseed alignment was set to 15; suppression of unpaired alignments as well as discordant alignments for paired reads; and suppression of unpaired reads to align against the reverse-complement (Crick) reference strand. Differential expression analysis of the sRNA-seq was done on allocated group comparison using EBSeq (v1.10.0). The investigators were blinded to the disease background of the group allocation. Differentially expressed miRs (DEmiRs) were defined as false discovery rate (FDR) < 0.05 and $|\text{fold change (FC)}| \geq 6$. Hierarchical clustering of DEmiRs between study groups was generated using Pearson correlation (subtracted from 1), and the algorithm was performed by Clustvis.^[25] Predicted miR targets and molecular pathways were generated using DIANA-TarBase v7 and DIANA-miRPath v3.0,^[26,27] respectively. Transcription factor (TF)–miR regulatory networks were predicted using TFmiR v1.2.^[28] Normalized expression of selected mature miRs ($\text{Log}_2[\text{total RPM}+1]$) in HCC tissues was also obtained from the Cancer Genome Atlas–Liver Hepatocellular Carcinoma (TCGA-LIHC) cohort using the UCSC Xena platform.^[29] Data were extracted from paired HCC tissue and the corresponding adjacent nontumoral liver tissue for analysis.

Cell line models and reagents

Human hepatic stellate cell line LX2 (SCC064) was purchased from MilliporeSigma. Immortalized human hepatocyte cell line MIHA was provided by Dr. Jayanta Roy-Chowdhury, Albert Einstein College of Medicine, New York. LX2 cells were maintained in Dulbecco's modified Eagle's medium (DMEM)–high glucose supplemented with 10% fetal bovine serum (FBS) and 1% penicillin–streptomycin (Gibco by Life Technologies). MIHA cells were maintained in DMEM–high glucose supplemented with 1 mM sodium pyruvate, 10% FBS, and 1% penicillin–streptomycin. All cells were cultured in a humidified incubator at 37°C with 5% CO_2 . Cell line was routinely checked and tested negative for mycoplasma contamination before use.

Cell transfection

miR mimic for hsa–miR-137-3p (Assay ID: MC10513) and negative control mimic (Cat# 4464058) were purchased from Thermo Fisher Scientific. PcDNA-DEST47-GFP-GFP was a gift from Patrick Van Oostveldt (Addgene plasmid #36139).^[30] pDEST-hMeCP2-GFP was a gift from Huda Zoghbi (Addgene plasmid #48078).^[31] pCMV-hERalpha was a gift from Elizabeth Wilson (Addgene plasmid #101141).^[32] Transient transfection of expression plasmids (1 μ g) and miR mimics (1 nm) was performed on LX2 or MIHA cells using Lipofectamine 2000 (Thermo Fisher

Scientific) according to the manufacturer's instruction. Transfected cells were harvested 24 h following transfection unless otherwise specified.

RNA extraction from cell line

Total RNA was isolated from cell lines using RNAiso Plus (Takara Bio Inc.) according to the manufacturer's protocol.

Reverse-transcription and quantitative PCR

For detection of miR, extracted small RNA was reverse-transcribed using Applied Biosystems Taqman miR reverse-transcription kit in conjunction with a miR-specific stem-loop primer according to the manufacturer's instructions (Thermo Fisher Scientific). Briefly, 10 ng of RNA was used as template, and primers from TaqMan microRNA assay (Cat# 4427975; Thermo Fisher Scientific) were used for each reverse-transcription reaction using Applied Biosystems ProFlex PCR System (Thermo Fisher Scientific). Complementary DNA samples were stored at -20°C before use. Quantitative PCR was performed using Taqman Universal PCR master mix (without UNG) and TaqMan probe and primers mix according to the manufacturer's protocol (Thermo Fisher Scientific). Assay was done using Applied Biosystems StepOnePlus real-time PCR system (Thermo Fisher Scientific). TaqMan miRNA assays used were as follows: hsa-miR-200a-5p (ID: 001011), hsa-miR-137-3p (ID: 001129), hsa-miR-34c-5p (ID: 000428), and small nucleolar RNA, C/D Box 44 (RNU44) (ID: 001094). Expression of miR of interest was normalized to RNU44. For protein coding genes and primary miR, RNA (500 ng) was reverse-transcribed using PrimeScript RT Master Mix (Takara). Quantitative PCR reaction was performed using Applied Biosystems Power SYBR Green PCR master mix (Thermo Fisher Scientific) on StepOne real-time PCR systems (Thermo Fisher Scientific) or the LightCycler 480 system (Roche Diagnostics). Primer sequences used are listed in Table S1. Expression of miRs or genes of interest was normalized to RNU44 or hypoxanthine-guanine phosphoribosyltransferase respectively. Relative expression of miRs/genes of interest was performed using the $2^{-\text{dCT}}$ or $2^{-\text{ddCT}}$ method. Data are presented as mean \pm SD of values from at least three independent experiments.

Statistical analysis

Two-tailed unpaired *t* test, Mann–Whitney U test, or Wilcoxon matched-pairs signed rank test was used to compare differences between two groups whenever

appropriate. Kruskal-Wallis test was used for comparison across more than two groups. Statistically compared groups showed similar variance. Diagnostic performance of hsa-miR-200a-5p and hsa-miR-34c-5p was determined by area under receiver operating characteristic curve (AUROC). $p < 0.05$ was considered as statistically significant. Statistical analyses were performed using GraphPad Prism V8.2.1 (GraphPad Software Inc.).

RESULTS

Clinicopathological characteristics of the study cohort

Liver tissues from 22 patients with HBV-associated cirrhosis (11 males and 11 females) were studied. Representative microscopic images of cirrhotic liver tissues are shown in Figure 1A. The clinicopathological parameters of the four groups, namely cirrhosis from males (cirrhosis-M), cirrhosis from females (cirrhosis-F), control from males (ctrl-M) and control from females (ctrl-F), are provided in Table S2. Raw data obtained from sRNA-seq underwent standard pipeline for quantification of mature miRs expression in each sample followed by identification of DEmiRs. We made use of the pathway enrichment analyses, downstream gene targets prediction, and TF-miR regulatory network to investigate the biological significance and their associated molecular mechanisms in HBV-associated cirrhotic liver. A simplified workflow from sample preparation to sRNA-seq is shown in Figure 1B.

miR expression profiles in HBV-associated cirrhosis display distinct patterns between males and females

Mean total throughput from the 32 samples was 7.2 Gb (range: 5.9–12.5 Gb). Filtered read pairs aligned to reference genome were counted, and the numbers of filtered read pairs mapped to mature miR were comparable between groups (Figure 2A). Mean percentage of filtered reads of all 32 samples was 87.9% (range: 72.3%–96.0%), whereas the mean percentage of filtered read pairs mapped to mature miR was 14.9% (range: 2.9%–29.7%). Percentage of filtered read pairs mapped to mature miR, hairpin miR, piwi-interacting RNA, ribosomal RNA, and unmapped read pairs of each sample were listed in Table S3. Total number of mature miR identified from the cirrhosis-M, cirrhosis-F, ctrl-M, and ctrl-F groups were 1836, 1830, 1479, and 1451, respectively. DEmiRs were defined as FDR < 0.05 and $|\text{FC}| \geq 6$. Between the ctrl-M and ctrl-F groups, no DEmiRs were identified. Between the cirrhosis-F and ctrl-F groups, 12 miRs (6 down-regulated, 6 up-regulated) were differentially expressed. Between the cirrhosis-M and ctrl-M

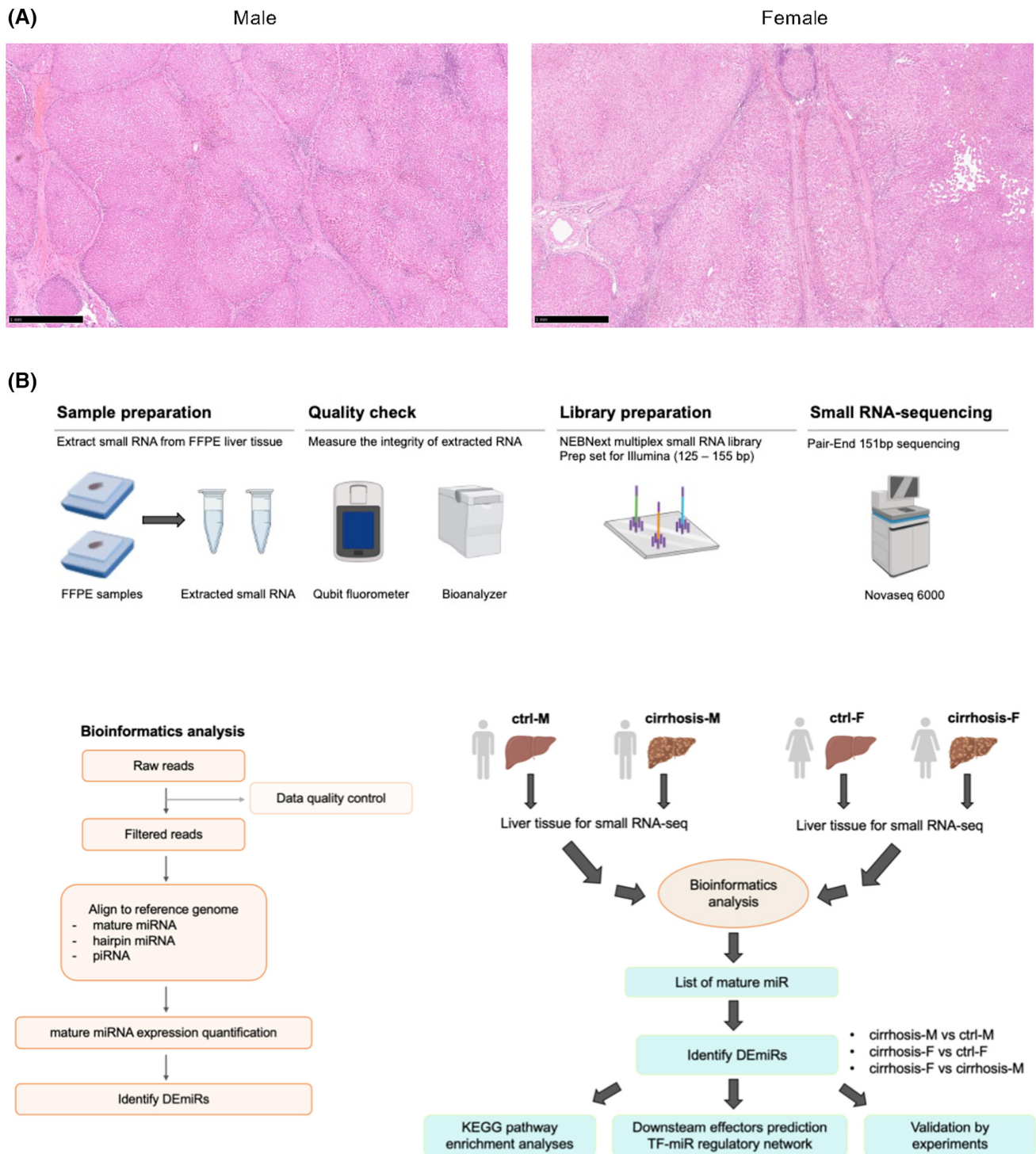


FIGURE 1 MicroRNA (miR) profiles in hepatitis B virus (HBV)-associated liver cirrhosis were analyzed by small RNA-sequencing. (A) Representative histological images of cirrhotic liver samples (magnification, $\times 25$; scale bar, 1 mm). (B) Illustration of the workflow from formalin-fixed paraffin-embedded (FFPE) tissue extraction to small RNA-sequencing (sRNA-seq; upper). Pipeline of bioinformatics analysis adopted in the sRNA-seq results (lower left). Summary of the study concept to investigate the biological significance conferred by the differentially expressed miRNAs (DEmiRs) in HBV-associated cirrhotic liver between females and males (lower right). Images created with [BioRender.com](https://www.biorender.com). Abbreviations: cirrhosis-F, cirrhosis from female; cirrhosis-M, cirrhosis from male; ctrl-F, control from female; ctrl-M, control from male; KEGG, Kyoto Encyclopedia of Genes and Genomes; piRNA, piwi-interacting RNA; TF-miR, transcription factor-miRNA

groups, 65 miRs (1 down-regulated, 64 up-regulated) were identified as DEmiRs. Twenty-six miRs were differentially expressed (23 down-regulated, 3 up-regulated

in cirrhosis-F) between the cirrhosis-F and cirrhosis-M groups. By comparing all groups with cirrhosis with control samples, 45 DEmiRs (4 down-regulated, 41

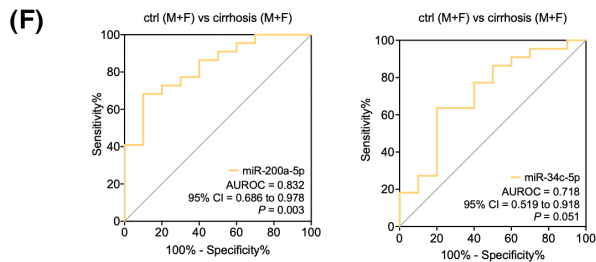
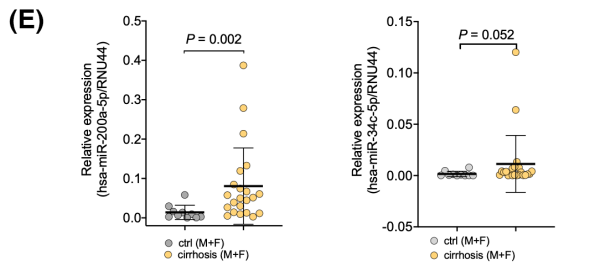
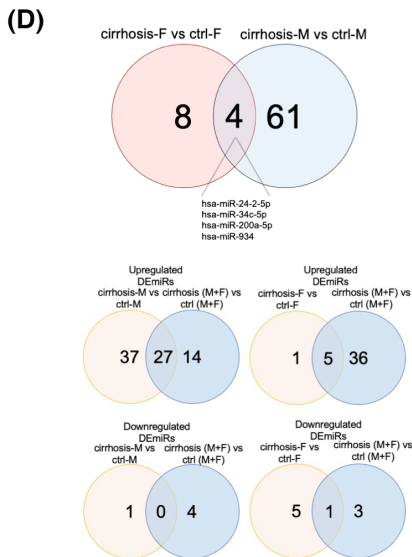
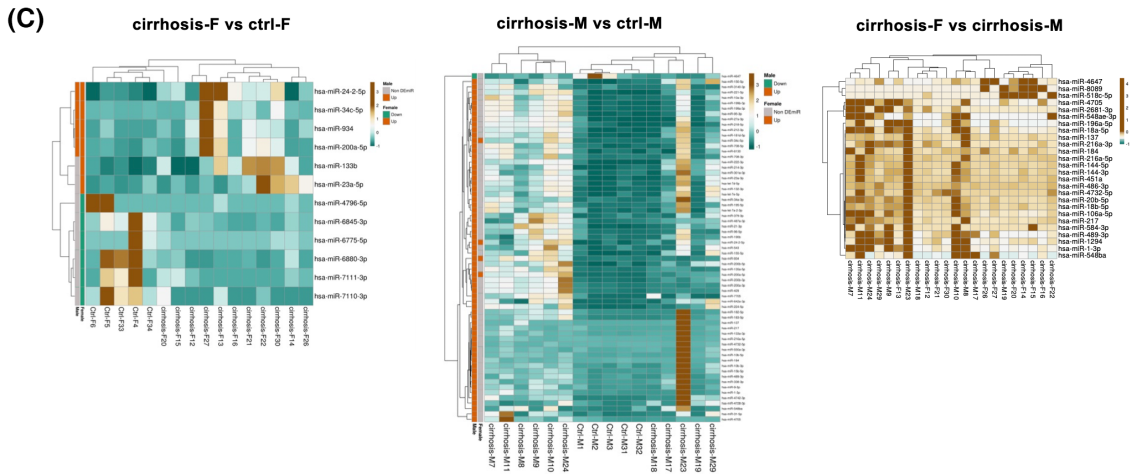
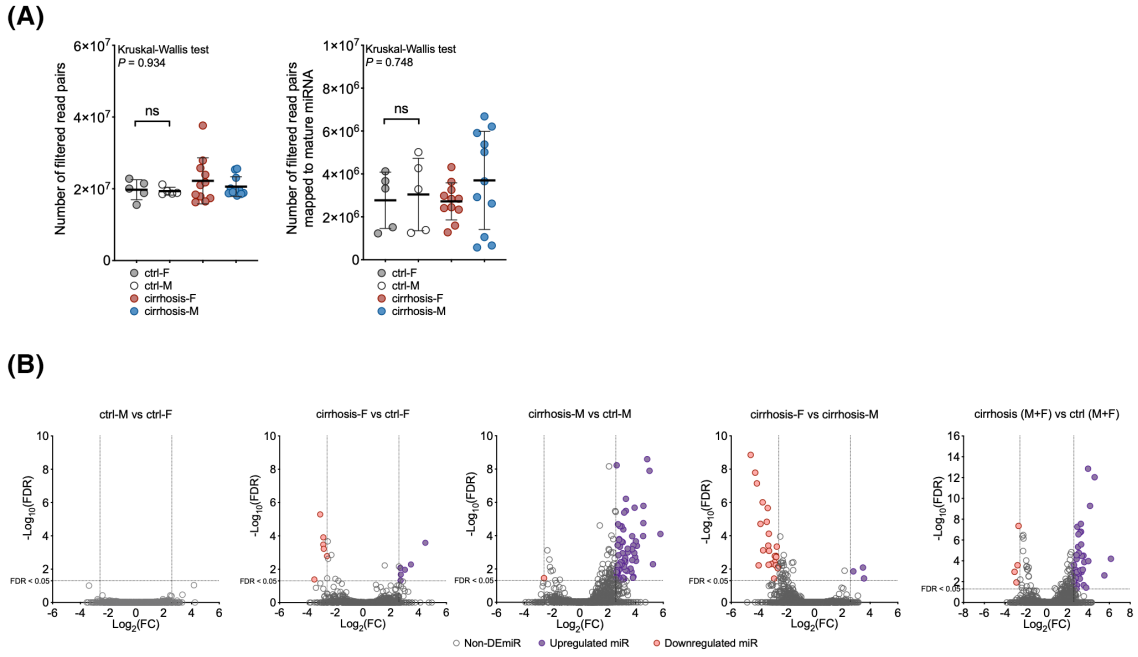


FIGURE 2 DE miRs in HBV-associated cirrhosis were identified by group comparisons. (A) Comparison of the number of filtered read pairs after sRNA-seq among all groups (left). Comparison of the number of filtered read pairs mapped to mature miR among all groups (right): ctrl-M, n = 5; ctrl-F, n = 5; cirrhosis-M, n = 11; and cirrhosis-F, n = 11. Kruskal-Wallis test was performed for comparison between multiple groups. Mann-Whitney U test was performed for comparison between two groups. Mean \pm SD are graphed. (B) Left to right: Volcano plots depicting the distribution of the DE miRs in each paired group comparison: ctrl-M versus ctrl-F, cirrhosis-F versus ctrl-F, cirrhosis-M versus ctrl-M, cirrhosis-F versus cirrhosis-M, and cirrhosis (M+F) versus ctrl (M+F). Empty dot, non-differentially expressed miR; purple dot, up-regulated miR; pink dot, down-regulated miR. (C) Heatmaps of the DE miRs in each paired group of comparison performed by Clustvis: cirrhosis-F versus ctrl-F, cirrhosis-M versus ctrl-M, and cirrhosis-F versus cirrhosis-M. DE miRs and non-DE miRs colored in boxes are shown on the left of the heatmaps: orange, up-regulated miR; green, down-regulated miRs; and gray, non-DE miRs. Color of non-DE miRs boxes was modified using GIMP (v2.10.24). (D) Venn diagram showing the four common DE miRs in both sex groups with cirrhotic liver when compared with the respective control groups (upper). Venn diagram showing the DE miRs overlapping in each group of comparison: cirrhosis-M versus ctrl-M to cirrhosis (M+F) versus ctrl (M+F) (lower left) and cirrhosis-F versus ctrl-F to cirrhosis (M+F) versus ctrl (M+F) (lower right). (E) Validation of miR-200a-5p and miR-34c-5p expression in FFPE tissue of the same cohort by quantitative polymerase chain reaction (PCR): ctrl (M+F), n = 5 male/n = 5 female; and cirrhosis (M+F), n = 11 male/11 female. Relative-expression data are normalized to small nucleolar RNA, C/D Box 44 (RNU44); Mann-Whitney U test. Data are presented as mean \pm SD. (F) Receiver operating characteristic (ROC) curve of miR-200a-5p and miR-34c-5p in detecting patients with cirrhotic liver from normal liver. *p* value, 95% confidence interval (CI), and area under ROC (AUROC) are shown on the graph: ctrl (M+F), n = 5 male/5 female; and cirrhosis (M+F), n = 11 male/11 female. Abbreviations: F, female; FC, fold change; FDR, false discovery rate; M, male; ns, not significant

TABLE 1 Top 10 DE miRs identified in group with cirrhosis versus control group for each sex

	miR ID	miR name	Fold change	Regulation type	FDR
cirrhosis-F vs. ctrl-F	MIMAT0000686	hsa-miR-34c-5p ^a	22.327	Up	0.000
	MIMAT0019970	hsa-miR-4796-5p	11.334	Down	0.041
	MIMAT0004977	hsa-miR-934 ^a	10.879	Up	0.005
	MIMAT0027661	hsa-miR-6880-3p	8.491	Down	0.000
	MIMAT0004496	hsa-miR-23a-5p	8.075	Up	0.011
	MIMAT0028118	hsa-miR-7110-3p	7.265	Down	0.000
	MIMAT0027591	hsa-miR-6845-3p	7.239	Down	0.000
	MIMAT0027450	hsa-miR-6775-5p	7.095	Down	0.001
	MIMAT0001620	hsa-miR-200a-5p ^a	6.565	Up	0.021
	MIMAT0004497	hsa-miR-24-2-5p ^a	6.495	Up	0.047
cirrhosis-M vs. ctrl-M	MIMAT0000429	hsa-miR-137	55.552	Up	7.91E-05
	MIMAT0019873	hsa-miR-4742-3p	38.201	Up	5.21E-03
	MIMAT0001620	hsa-miR-200a-5p ^a	32.236	Up	1.27E-08
	MIMAT0000281	hsa-miR-224-5p	28.706	Up	2.54E-09
	MIMAT0000686	hsa-miR-34c-5p ^a	23.782	Up	1.62E-06
	MIMAT0000428	hsa-miR-135a-5p	23.676	Up	1.76E-05
	MIMAT0004977	hsa-miR-934 ^a	23.390	Up	1.06E-04
	MIMAT0000416	hsa-miR-1-3p	17.146	Up	4.04E-04
	MIMAT0000454	hsa-miR-184	16.407	Up	3.27E-03
	MIMAT0020924	hsa-miR-642a-3p	16.258	Up	2.20E-04

^aCommonly deregulated miR identified in males and female.

up-regulated) were identified (Figure 2B). Heatmaps with hierarchical clustering were constructed based on DE miRs identified between specific groups (cirrhosis-F and ctrl-F, cirrhosis-M and ctrl-M, and cirrhosis-F and cirrhosis-M) (Figure 2C). The top 10 DE miRs found in the cirrhotic liver group when compared with the respective control of each sex are summarized in Table 1. To understand whether cirrhotic livers from both sexes share a list of similar DE miRs, we compared the lists of DE miRs and found that only four miRs (miR-24-2-5p, miR-34c-5p, miR-200a-5p, and miR-934) were

commonly deregulated in both groups with cirrhosis. These DE miRs were up-regulated in the cirrhotic liver groups when compared with their respective control groups. To further highlight, most of the DE miRs were specifically deregulated in one sex only (Figure 2D). The numbers of DE miRs and degree of miR alteration in terms of FC in the male group appeared to be much higher than that in the female group. A cross comparison between the lists of DE miRs identified in cirrhosis-M versus ctrl-M, cirrhosis-F versus ctrl-F, and cirrhosis (M+F) versus ctrl (M+F) was also performed. Analyses

showed that 27 (of 64 DEmiRs from male-only comparison and of 41 DEmiRs from M+F comparison) and 5 (of 6 DEmiRs from female-only comparison and of 41 DEmiRs from M+F comparison) were commonly up-regulated. None (of 1 DEmiRs from male-only comparison and of 4 DEmiRs from M+F comparison) and 1 (of 6 DEmiRs from female-only comparison and of 4 DEmiRs from M+F comparison) were commonly down-regulated (Figure 2D). These findings suggest that HBV-associated cirrhosis bears distinct deregulated miR expression patterns in males and females. Expression of miR-200a-5p and miR-34c-5p in the same cohort was evaluated by quantitative PCR (Figure 2E). With AUROC analysis, both miR-200a-5p and miR-34c-5p appeared to be a good marker (AUROC = 0.832 and 0.718, respectively) to differentiate HBV-associated cirrhosis from controls (Figure 2F).

Prediction analyses highlight potential sex-specific molecular mechanisms and regulators in HBV-associated cirrhosis

First, Kyoto Encyclopedia of Genes and Genomes pathway enrichment analyses were performed based on the 65 DEmiRs and 12 DEmiRs identified in cirrhosis-M and cirrhosis-F, respectively (cirrhosis vs. control groups in each sex). Gene targets of these DEmiRs were derived from DIANA-Tarbase v7.0, which gene targets and miRs interactions were experimentally validated, and subsequent pathway enrichment analyses were conducted using DIANA-miPath v3 (Figure 3A). Although certain pathways are commonly deregulated in both males and females, including proteoglycans in cancer, cell cycle, viral carcinogenesis, adherens junction, and TGF- β signaling pathway, some human pathological processes related pathways were only highlighted in one sex. For example, fatty acid biosynthesis was highlighted in females, which was not identified in males. Contrarily, extracellular matrix–receptor interaction, p53 signaling pathway, Hippo signaling pathway, tumor necrosis factor signaling pathway, and the forkhead box O signaling pathway, for example, were specifically enriched in males. Apart from revealing the “sex-specific” DEmiR-associated molecular

pathways enriched in the groups with cirrhosis when compared with their respective control groups, DEmiRs and the biological significance of these DEmiRs in the cirrhotic liver between females and males (cirrhosis-F vs. cirrhosis-M) were also determined. This comparison was made to evaluate the molecular differences between females and males with the same disease. The top five DEmiRs (miR-486-3p, miR-216a-5p, miR-144-5p, miR-2681-3p, and miR-137) were all down-regulated in the cirrhotic-F group (Table 2). We further identified downstream effectors of these five DEmiRs using DIANA-Tarbase v.7. Ribosomal protein S27 like (*RPS27L*) was the sole target of three DEmiRs, namely miR-137, miR-144-5p, and miR-486-3p (Figure 3B). Liver disease–associated TF-miR network was constructed to determine the upstream regulators of identified DEmiRs (cirrhosis-F vs. cirrhosis-M) using TFmiR database. Methyl CpG binding protein 2 (*MECP2*) and estrogen receptor 1 (*ESR1*) were highlighted as potential transcription regulators of the DEmiRs (*MECP2* on miR-184 and miR-137; *ESR1* on miR-18a, miR-106a, miR-18b, and miR-20b). Hepatic stellate cells are recognized to be a major cell type implicated in liver fibrogenesis with their role in extracellular matrix production during liver injury and regeneration. In an attempt to verify the prediction, *MECP2* and *ESR1* were each over-expressed in LX2 cells, and expression of the respective primary miRs were examined. Up-regulation of primary miR-137 and miR-184 was observed following overexpression of *MECP2* (at 24 h after transfection), whereas overexpression of *ESR1* did not alter all predicted miRs (Figure 3C). To evaluate the involvement of normal hepatocytes in this regulation, MIHA cells were also adopted to examine the expression of primary miR-137 and miR-184. The results showed that expression of these miRs was not significantly altered in *MECP2*-overexpressing MIHA cells (Figure S1).

Sex-specific DEmiRs in HBV-associated cirrhosis carry potential functional significance

As some DEmiRs were only identified in the male but not the female group (Table 1), we questioned what

FIGURE 3 Potential dysregulated signaling pathways, upstream regulators, and downstream effectors were predicted based on the DEmiRs. (A) KEGG pathways enriched by the DEmiRs identified in cirrhosis male group ($n = 11$) or cirrhosis female group ($n = 11$) when compared with their respective controls ($n = 5$ male/5 female). Analyses were performed using DIANA-miRPath v.3. Pathways commonly enriched in both genders are highlighted in orange. (B) Venn diagram illustrated the common downstream predicted target genes of DEmiRs in cirrhosis female group when compared with cirrhosis male group. The sole target, ribosomal protein S27 like, of miR-137, miR-486-3p, and miR-144-5p is highlighted in red. (C) Validation of methyl CpG binding protein 2 (*MECP2*) and estrogen receptor 1 (*ESR1*) expression in *MECP2*-expression plasmid ($n = 3$) and *ESR1*-expression plasmid ($n = 5$) transfected LX2 cells (left panels). Relative expression data are normalized to hypoxanthine-guanine phosphoribosyltransferase (*HPRT*). Expression of primary miR-137 and miR-184 following overexpressing *MECP2* in LX2 cells ($n = 3$) (right upper panel). Expression of primary miR-18a, miR-18b, miR-20b, and miR-106a following overexpression of *ESR1* in LX2 cells ($n = 5$) (right lower panel). Relative expression data are normalized to RNU44; two-tailed unpaired t test. Data are presented as mean \pm SD; * $p < 0.05$ and ** $p < 0.01$. Abbreviations: AMPK, adenosine monophosphate–activated protein kinase; ECM, extracellular matrix; MAPK, mitogen-activated protein kinase; mRNA, messenger RNA; mTOR, mammalian target of rapamycin; TGF- β , transforming growth factor β ; TNF, tumor necrosis factor; HTLV, human T-cell leukemia virus

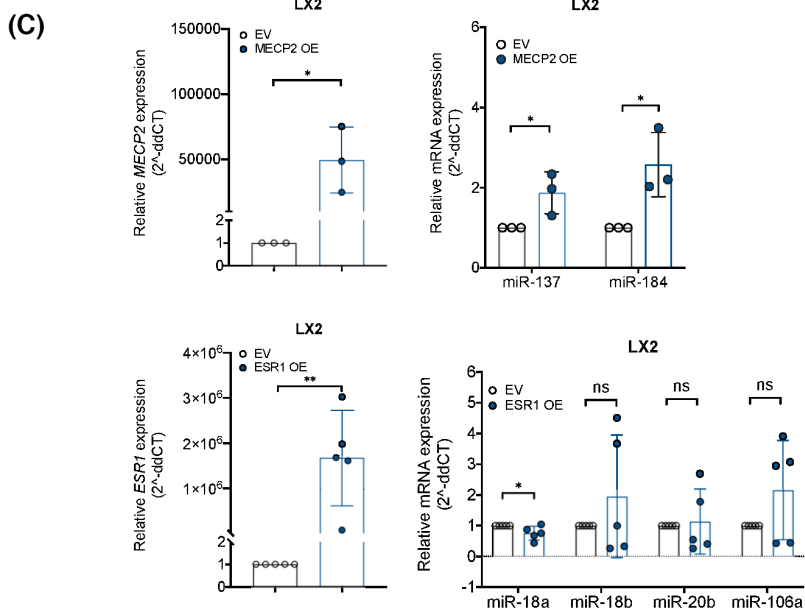
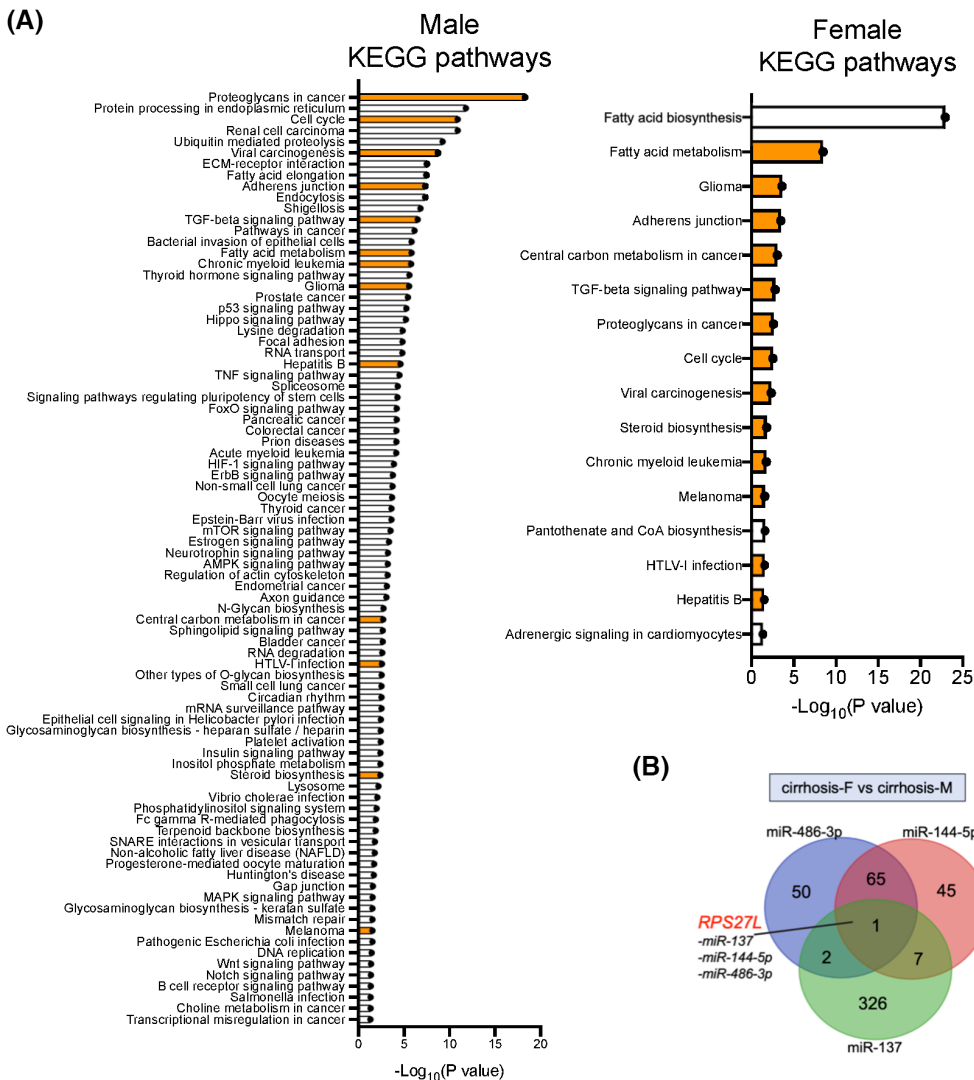


TABLE 2 Top 5 DEmiRs identified in cirrhosis female group compared with cirrhosis male group

	miR ID	miR name	Fold change	Regulation type	FDR
cirrhosis-F vs. cirrhosis-M	MIMAT0004762	hsa-miR-486-3p	24.251	Down	1.39E-09
	MIMAT0000273	hsa-miR-216a-5p	19.331	Down	1.62E-08
	MIMAT0004600	hsa-miR-144-5p	17.777	Down	7.16E-08
	MIMAT0013516	hsa-miR-2681-3p	16.279	Down	0.006
	MIMAT0000429	hsa-miR-137	14.855	Down	1.93E-05

Note: In the present study, we demonstrated the distinct miR expression patterns in HBV-associated cirrhosis between sexes using sRNA-seq. Prediction of upstream and downstream regulators based on the DEmiRs suggests sex-specific molecular mechanisms implicated in the pathogenesis and biological behavior of liver cirrhosis.

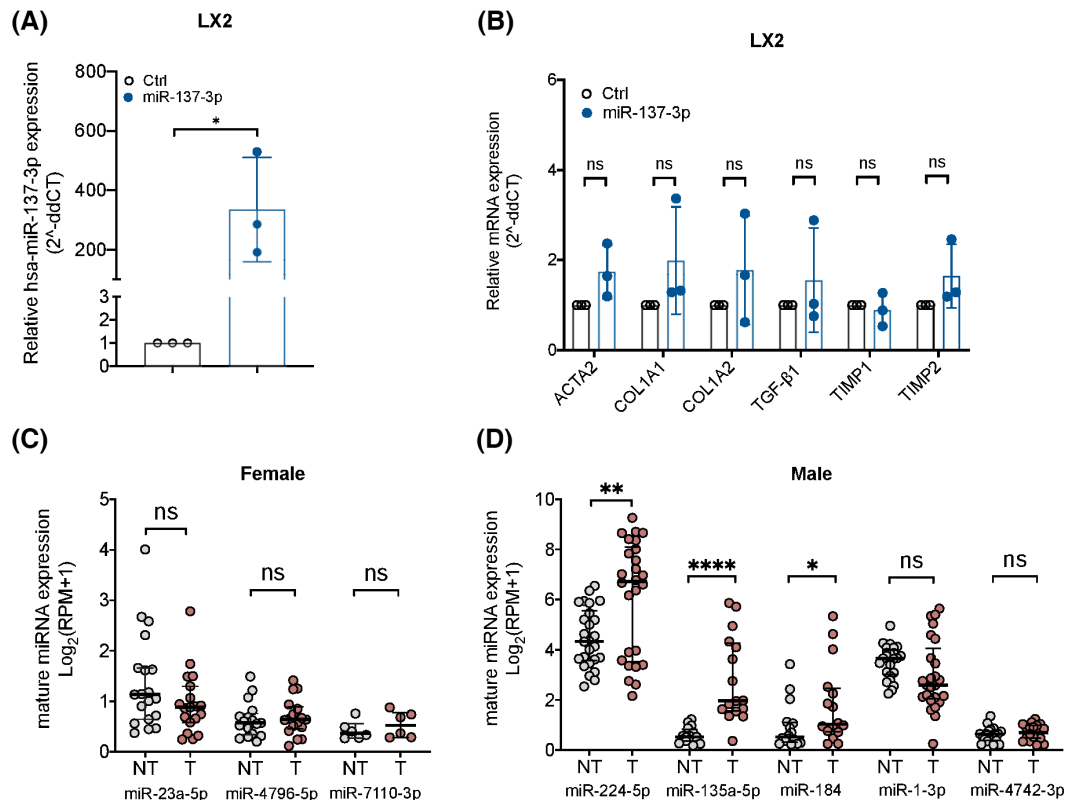


FIGURE 4 Functional significance of sex-specific DEmiRs was explored. (A) Validation of miR-137-3p expression in miR-137-3p mimic (1 nM) transfected LX2 cells. Relative expression data are normalized to RNU44 (n = 3); two-tailed unpaired *t* test. Data are presented as mean ± SD. (B) mRNA expression of fibrogenic genes smooth muscle actin alpha 2, collagen type I alpha 1, *COL1A2*, *TGF-β1*, *TIMP1*, and *TIMP2* following transfecting miR-137-3p mimic (1 nM) in LX2 cells (n = 3). Relative expression data are normalized to *HPRT*; two-tailed unpaired *t* test. Data are presented as mean ± SD. (C) Expression of female-specific DEmiRs (miR-23a-5p [n = 19], miR-4796-5p [n = 17], and miR-7110-3p [n = 6]) in female paired hepatocellular carcinoma (HCC) tissues and nontumoral liver tissues obtained from The Cancer Genome Atlas–Liver Hepatocellular Carcinoma (TCGA-LIHC) data set; Wilcoxon matched-pairs signed-rank test. Data are presented as median with interquartile range (IQR). (D) Expression of male-specific DEmiRs (miR-224-5p [n = 26], miR-135a-5p [n = 16], miR-184 [n = 16], miR-1-3p [n = 25], and miR-4742-3p [n = 19]) in male paired HCC tissues and nontumoral liver tissues obtained from the TCGA-LIHC data set; Wilcoxon matched-pairs signed-rank test. Data are presented as median with IQR; **p* < 0.05, ***p* < 0.01, and *****p* < 0.0001. Abbreviations: NT, nontumoral liver tissues; T, HCC tumor tissues

functions these sex-specific DEmiRs may exert in the liver. Hepatic stellate cells are a major cell type implicated in liver fibrogenesis; thus, miR-137-3p mimic was used in LX2 cells to study its functional effects *in vitro*. Transfection efficiency was first confirmed

by quantitative PCR (Figure 4A). We quantified the expression of myofibroblast marker smooth muscle actin and fibrogenic markers collagen type I alpha 1 (*COL1A1*), *COL1A2*, *TGF-β1*, tissue inhibitor of metalloproteinase (*TIMP1*) and *TIMP2* by quantitative

PCR upon transfecting miR-137-3p mimic in LX2 cells (Figure 4B). From the results, the fibrogenic genes were not significantly altered in the miR-137-3p mimic-transfected cells. With further experiments, we found that expressions of fibrogenic genes smooth muscle actin alpha 2, *COL1A1*, *TGF- β 1*, and *TIMP2* were up-regulated at 48h (but not at 24h) following overexpression of MECP2, whereas expressions of miR-137 and miR-184 were not significantly altered at this time point (Figure S2). These findings suggest that miR-137-3p *per se* may not be sufficient to mediate the effect of MECP2 on hepatic stellate cells. To further explore the potential significance of the sex-specific DEmiRs in multistep hepatocarcinogenesis, we analyzed the expression of the top-listed DEmiRs identified in the cirrhosis-M versus control-M, as well as cirrhosis-F versus control-F comparison, from TCGA-LIHC data set. Some analyses were not feasible due to the small number of paired samples (which include miR-6880-3p, miR-6845-3p, miR-6775-5p, miR-137, and miR-642a-3p). Among the three female-specific DEmiRs, miR-23a-5p, miR-4796-5p and miR-7110-3p showed no significant difference in female HCC tumor tissues when compared with nontumoral liver tissues (Figure 4C). Among the five male-specific DEmiRs, miR-224-5p, miR-135a-5p and miR-184 (all up-regulated in cirrhosis vs. control) were up-regulated in male HCC tissues compared with nontumoral liver tissues, whereas miR-1-3p and miR-4742-3p showed no significant difference between groups (Figure 4D).

DISCUSSION

In this study, by using next generation sequencing, we performed a sex-specific analysis of the miR profiles with the liver tissue samples from HBV cirrhosis. Our findings showed that the deregulated miR profiles in male and female patients with cirrhosis are relatively distinct. The degree of deregulation was higher in males versus females as from the number of differentially expressed genes and number of predicted signaling pathways. Most of the DEmiRs in cirrhotic male samples were up-regulated, whereas half in the female counterpart were down-regulated. Common DEmiRs in both sexes constitute a minority. Our further computational and bioinformatics analyses also highlighted several signaling pathways, downstream effectors, and upstream regulators that potentially play a key role in the pathogenesis of liver cirrhosis in each sex. Analysis of the TCGA-LIHC data set suggested a role of sex-specific DEmiRs in multistep hepatocarcinogenesis.

We compared our findings with reports from expression analysis using clinical samples collected from patients with HBV. Among the DEmiRs in cirrhosis-M versus ctrl-M, cirrhosis-F versus ctrl-F, as

well as cirrhosis-F versus cirrhosis-M groups, only a small proportion have been reported in the studies on expression analysis, especially in the cirrhosis-F versus cirrhosis-M groups. With reference to two previous reports on miR profiling of HBV liver tissues by microarray,^[22,23] some of the DEmiRs were also identified in our current study, which mostly belong to the cirrhosis-M versus ctrl-M groups (for example, miR-150-5p, miR-155-5p, miR-200a-3p, miR-200b-3p, miR-338-3p, and miR-642a-3p as revealed by Chen et al. in the S4 versus S0 group^[22]; and miR-96-5p, miR-1-3p, miR-10b-5p, miR-218-5p, and miR-23a-3p as shown by Singh et al. in their analysis between advanced fibrosis and early fibrosis groups^[23]). On comparing the DEmiRs identified in different group comparisons, the pattern of DEmiRs identified in cirrhosis-F versus cirrhosis-M was not readily discernible in the cirrhosis-M or cirrhosis-F versus the respective control group in the same sex. This was likely due to the different reference groups used in the comparisons (cirrhotic-M and ctrl-M/ctrl-F, respectively).

Some of the top-listed DEmiRs identified in our current study were reported to show profibrotic functions using cell line models (e.g., miR-34c^[33,34] and miR-23a^[35,36]). The top-ranking male-specific miR identified in our study, miR-137, was not reported to exert any pro-fibrogenic functions thus far. Consistently, expression of fibrogenic genes was not altered in LX2 cells following miR-137 transfection from our *in vitro* experiments. Likewise, miR-486-3p and miR-216a-5p, identified from the cirrhosis-F versus cirrhosis-M analysis, were not reported to result in liver fibrosis from functional studies. Of note, while miR-200a was up-regulated in cirrhotic liver tissues, its functional role in the previous reports appeared incongruent. In multiple studies it was demonstrated that miR-200a exerts antifibrotic functions in the liver.^[37,38] Moreover, DEmiRs in the cirrhosis-F group (vs. ctrl-F), such as miR-934, may not have any predicted gene target, rendering the uncertainty of its functional significance. These observations may imply that the miR network is complex in cirrhosis and the functional phenotype may rely on an interplay between multiple markers.

Fatty acid biosynthesis pathway was identified as a deregulated signaling pathway in cirrhosis-F group (vs. ctrl-F) but not in the male counterpart, suggesting that fatty acid synthesis may still play an important role in liver fibrogenesis among female patients with primary etiology other than fatty liver disease. Apart from nonneoplastic conditions, fatty acid biosynthesis pathway has been found to facilitate tumorigenesis via multiple mechanisms.^[39,40] Moreover, target prediction analysis showed that *RPS27L* is a common target for the DEmiRs being down-regulated in cirrhotic-F when compared with the cirrhotic-M group. *RPS27L* encodes

a ribosomal protein and was reported to suppress tumorigenesis by directly regulating p53.^[41] These findings suggest that *RPS27L* may be a factor accounting for lower malignant transformation potential in female cirrhosis. The identified DE miRs by comparing cirrhosis-F versus cirrhosis-M highlighted *ESR1* and *MeCP2* as potential upstream master regulators. From our experiments, we could validate the regulation of DE miRs following overexpressing *MECP2* but not *ESR1* in LX2 cells. Of note, *MeCP2* was reported as a regulator of miRs/genes involved in liver fibrosis.^[42–44] Regarding results on *ESR1*, we speculate that its effect on miR regulation may also depend on estrogen level in the cells. Because LX2 is a male cell line, the regulation of *ESR1* on sex-specific DE miRs may not be fully characterized by manipulation of gene targets alone.

Our study could provide some insights on sex-specific biomarkers to monitor the progression of liver fibrosis (e.g., miR-137, miR-4742-3p, and miR-224-5p for male patients and miR-4796-5p, miR-6880-3p, and miR-23a-5p for female patients). The great magnitude of miRs and signaling pathway derangement may explain the high risk of liver fibrosis progression in males. In addition, the differential predicted upstream regulators and downstream effectors between the two sexes, such as fatty acid biosynthesis pathway, *RPS27L*, *ESR1* and *MeCP2*, may offer insights in explaining the sex difference in disease course and in devising antifibrotic therapeutics for different patient groups. By referring to the expressions of some DE miRs from the TCGA-LIHC data set, we might be able to gather some insight on the functions of sex-specific DE miRs. For the female-specific DE miRs, none (of the 3) female-specific DE miRs was deregulated in female HCC, whereas 3 (of the 5) up-regulated male-specific DE miRs identified in our study were also up-regulated in male HCC. While miR-224-5p and miR-135a-5p were also up-regulated in female HCC versus nontumor tissue, concordant changes were not observed in the cirrhosis versus normal comparison. These findings suggest that male-specific DE miRs may play a functional role in the multistep events of tumor development. One merit of our study is the use of next generation sequencing in the identification of miRs from clinical samples. In a previous report, miR changes were studied with next generation sequencing of hepatitis C liver tissues.^[45] For HBV, miR profiling was mostly performed with microarray method in previous studies.^[22,23] A limitation of our study is the cohort size, which was largely due to the number of female cirrhosis cases falling into the inclusion criteria. Clinicopathological parameters (e.g., age, albumin, bilirubin levels) may constitute confounding effects in the analysis of DE miRs. Expansion of the study cohort or inclusion of samples with other primary liver disease etiologies for group comparison could allow a more comprehensive analysis. Another limitation is the lack of validation of target gene predictions by real-time

quantitative PCR. The samples were extracted from FFPE tissues and contained fragmented RNAs with a major peak below 200 nucleotides (range: 40%–96% of total). The fragmented size rendered gene-expression quantification suboptimal from a technical point of view.

Sex disparity has been observed in some human diseases, both neoplastic and nonneoplastic. The disparity includes incidence, pathogenic mechanisms, and biological behavior. It is therefore an important aspect to be addressed in the study of human diseases. Results from our study elaborated the commonly deregulated miRs and sex-specific DE miRs in HBV-associated cirrhosis. The former potentially represent some critical genetic events in cirrhosis, while the latter likely explain the sex disparity in the susceptibility and biological cause of CLD. Identification of these miRs together with their molecular mechanisms will help enrich our understanding of the genetic complexity of HCC. Based on our results, sex-specific serum miR markers could potentially be identified and validated for disease monitoring and risk stratification in patients with HBV. Despite the disparities between hepatic and blood miR expressions from some studies, some miRs were identified to show concordant differential expression patterns in tissue and blood samples from patients with liver fibrosis. To highlight, a positive correlation was observed between the expression of hepatic miR-122, miR-222, miR-33a, and miR-571 with corresponding serum levels.^[46–50] Hence, evaluation of a tissue-serum expression correlation for specific miRs is indicated. Moreover, sex-specific molecular targets could be of value for further studies to delineate the potential points of intervention more precisely, which hopefully will contribute to improve the prognosis of CLD.

AUTHOR CONTRIBUTIONS

Data acquisition: Kristy Kwan-Shuen Chan, Kwan-Yung Au, Wai-Ching Fung, Cheuk-Yan Wong, Albert Chi-Yan Chan, and Regina Cheuk-Lam Lo. *Data analysis:* Kristy Kwan-Shuen Chan, Kwan-Yung Au, and Regina Cheuk-Lam Lo. *Data interpretation:* Kristy Kwan-Shuen Chan, Kwan-Yung Au, and Regina Cheuk-Lam Lo. *Manuscript draft:* Kristy Kwan-Shuen Chan and Regina Cheuk-Lam Lo. *Statistical analysis:* Kristy Kwan-Shuen Chan. *Study concept, design, and supervision:* Regina Cheuk-Lam Lo.

ACKNOWLEDGMENT

The authors thank the Center for PanorOmic Sciences and Faculty Core Facility, LKS Faculty of Medicine, The University of Hong Kong, for their technical support. They also thank Dr. Jack Wong (Department of Pathology, HKU) for the technical advice. The results in this study are in part based on data generated by the TCGA Research Network: <https://www.cancer.gov/tcga>.

CONFLICT OF INTEREST

Nothing to report.

ORCID

Regina Cheuk-Lam Lo  <https://orcid.org/0000-0001-6213-0343>

REFERENCES

1. Fattovich G, Bortolotti F, Donato F. Natural history of chronic hepatitis B: special emphasis on disease progression and prognostic factors. *J Hepatol*. 2008;48:335–52.
2. Ma KW, Chok KSH, Fung JYY, Lo CM. Liver transplantation for hepatitis B virus-related hepatocellular carcinoma in Hong Kong. *J Clin Transl Hepatol*. 2018;6:283–8.
3. Zhang CY, Yuan WG, He P, Lei JH, Wang CX. Liver fibrosis and hepatic stellate cells: etiology, pathological hallmarks and therapeutic targets. *World J Gastroenterol*. 2016;22:10512–22.
4. Brunner SF, Roberts ND, Wylie LA, Moore L, Aitken SJ, Davies SE, et al. Somatic mutations and clonal dynamics in healthy and cirrhotic human liver. *Nature*. 2019;574:538–42.
5. Guy J, Peters MG. Liver disease in women: the influence of gender on epidemiology, natural history, and patient outcomes. *Gastroenterol Hepatol (N Y)*. 2013;9:633–9.
6. Ruggieri A, Gagliardi MC, Anticoli S. Sex-dependent outcome of hepatitis B and C viruses infections: synergy of sex hormones and immune responses? *Front Immunol*. 2018;9:2302.
7. Liu M, Tseng TC, Jun DW, Yeh ML, Trinh H, Wong GLH, et al. Transition rates to cirrhosis and liver cancer by age, gender, disease and treatment status in Asian chronic hepatitis B patients. *Hepatol Int*. 2021;15:71–81.
8. Evans AA, Chen G, Ross EA, Shen FM, Lin WY, London WT. Eight-year follow-up of the 90,000-person Haimen City cohort: I. Hepatocellular carcinoma mortality, risk factors, and gender differences. *Cancer Epidemiol Biomarkers Prev*. 2002;11:369–76.
9. Lee CM, Lu SN, Changchien CS, Yeh CT, Hsu TT, Tang JH, et al. Age, gender, and local geographic variations of viral etiology of hepatocellular carcinoma in a hyperendemic area for hepatitis B virus infection. *Cancer*. 1999;86:1143–50.
10. Taylor BC, Yuan JM, Shamliyan TA, Shaikat A, Kane RL, Wilt TJ. Clinical outcomes in adults with chronic hepatitis B in association with patient and viral characteristics: a systematic review of evidence. *Hepatology*. 2009;49:S85–95.
11. Yeluru A, Nguyen P, Le AK, Zhao C, Hoang J, Yasukawa LA, et al. Gender differences in outcomes of cirrhosis in a large cohort of patients in the United States. *Gastroenterology*. 2017;152:S1142.
12. Zhu ZZ, Wang D, Cong WM, Jiang H, Yu Y, Wen BJ, et al. Sex-related differences in DNA copy number alterations in hepatitis B virus-associated hepatocellular carcinoma. *Asian Pac J Cancer Prev*. 2012;13:225–9.
13. Yu MW, Cheng SW, Lin MW, Yang SY, Liaw YF, Chang HC, et al. Androgen-receptor gene CAG repeats, plasma testosterone levels, and risk of hepatitis B-related hepatocellular carcinoma. *J Natl Cancer Inst*. 2000;92:2023–8.
14. Yu MW, Yang YC, Yang SY, Cheng SW, Liaw YF, Lin SM, et al. Hormonal markers and hepatitis B virus-related hepatocellular carcinoma risk: a nested case-control study among men. *J Natl Cancer Inst*. 2001;93:1644–51.
15. Chen PJ, Yeh SH, Liu WH, Lin CC, Huang HC, Chen CL, et al. Androgen pathway stimulates microRNA-216a transcription to suppress the tumor suppressor in lung cancer-1 gene in early hepatocarcinogenesis. *Hepatology*. 2012;56:632–43.
16. Gao P, Wong CC, Tung EK, Lee JM, Wong CM, Ng IO. Deregulation of microRNA expression occurs early and accumulates in early stages of HBV-associated multistep hepatocarcinogenesis. *J Hepatol*. 2011;54:1177–84.
17. Murakami Y, Yasuda T, Saigo K, Urashima T, Toyoda H, Okanoue T, et al. Comprehensive analysis of microRNA expression patterns in hepatocellular carcinoma and non-tumorous tissues. *Oncogene*. 2006;25:2537–45.
18. Szabo G, Bala S. MicroRNAs in liver disease. *Nat Rev Gastroenterol Hepatol*. 2013;10:542–52.
19. Barwari T, Eminaga S, Mayr U, Lu R, Armstrong PC, Chan MV, et al. Inhibition of profibrotic microRNA-21 affects platelets and their releasate. *JCI Insight*. 2018;3:e123335.
20. Ladeiro Y, Couchy G, Balabaud C, Bioulac-Sage P, Pelletier L, Rebouissou S, et al. MicroRNA profiling in hepatocellular tumors is associated with clinical features and oncogene/tumor suppressor gene mutations. *Hepatology*. 2008;47:1955–63.
21. Zheng B, Zhu YJ, Wang HY, Chen L. Gender disparity in hepatocellular carcinoma (HCC): multiple underlying mechanisms. *Sci China Life Sci*. 2017;60:575–84.
22. Chen R, Wu JC, Liu T, Qu Y, Lu LG, Xu MY. MicroRNA profile analysis in the liver fibrotic tissues of chronic hepatitis B patients. *J Dig Dis*. 2017;18:115–24.
23. Singh AK, Rooge SB, Varshney A, Vasudevan M, Bhardwaj A, Venugopal SK, et al. Global microRNA expression profiling in the liver biopsies of hepatitis B virus-infected patients suggests specific microRNA signatures for viral persistence and hepatocellular injury. *Hepatology*. 2018;67:1695–709.
24. Lo RC, Kim H. Histopathological evaluation of liver fibrosis and cirrhosis regression. *Clin Mol Hepatol*. 2017;23:302–7.
25. Metsalu T, Vilo J. ClustVis: a web tool for visualizing clustering of multivariate data using Principal Component Analysis and heatmap. *Nucleic Acids Res*. 2015;43:W566–70.
26. Vlachos IS, Paraskevopoulou MD, Karagkouni D, Georgakilas G, Vergoulis T, Kanellos I, et al. DIANA-TarBase v7.0: indexing more than half a million experimentally supported miRNA:mRNA interactions. *Nucleic Acids Res*. 2015;43:D153–9.
27. Vlachos IS, Zagganas K, Paraskevopoulou MD, Georgakilas G, Karagkouni D, Vergoulis T, et al. DIANA-miRPath v3.0: deciphering microRNA function with experimental support. *Nucleic Acids Res*. 2015;43:W460–6.
28. Hamed M, Spaniol C, Nazarieh M, Helms V. TFmiR: a web server for constructing and analyzing disease-specific transcription factor and miRNA co-regulatory networks. *Nucleic Acids Res*. 2015;43:W283–8.
29. Goldman MJ, Craft B, Hastie M, Repecka K, McDade F, Kamath A, et al. Visualizing and interpreting cancer genomics data via the Xena platform. *Nat Biotechnol*. 2020;38:675–8.
30. Dieriks B, Van Oostveldt P. Spatiotemporal behavior of nuclear cyclophilin B indicates a role in RNA transcription. *Int J Mol Med*. 2012;29:1031–8.
31. Baker SA, Chen L, Wilkins AD, Yu P, Lichtarge O, Zoghbi HY. An AT-hook domain in MeCP2 determines the clinical course of Rett syndrome and related disorders. *Cell*. 2013;152:984–96.
32. Mao C, Patterson NM, Cherian MT, Aninye IO, Zhang C, Montoya JB, et al. A new small molecule inhibitor of estrogen receptor alpha binding to estrogen response elements blocks estrogen-dependent growth of cancer cells. *J Biol Chem*. 2008;283:12819–30.
33. Li B, Liu J, Xin X, Zhang L, Zhou J, Xia C, et al. MiR-34c promotes hepatic stellate cell activation and liver fibrogenesis by suppressing ACSL1 expression. *Int J Med Sci*. 2021;18:615–25.
34. Li X, Chen Y, Wu S, He J, Lou L, Ye W, et al. microRNA-34a and microRNA-34c promote the activation of human hepatic stellate cells by targeting peroxisome proliferator-activated receptor gamma. *Mol Med Rep*. 2015;11:1017–24.
35. Brea R, Motino O, Frances D, Garcia-Monzon C, Vargas J, Fernandez-Velasco M, et al. PGE2 induces apoptosis of hepatic stellate cells and attenuates liver fibrosis in mice by

- downregulating miR-23a-5p and miR-28a-5p. *Biochim Biophys Acta Mol Basis Dis.* 2018;1864:325–37.
36. Dong Z, Li S, Si L, Ma R, Bao L, Bo A. Identification lncRNA LOC102551149/miR-23a-5p pathway in hepatic fibrosis. *Eur J Clin Invest.* 2020;50:e13243.
 37. Ezhilarasan D. MicroRNA interplay between hepatic stellate cell quiescence and activation. *Eur J Pharmacol.* 2020;885:173507.
 38. Hu BL, Shi C, Lei RE, Lu DH, Luo W, Qin SY, et al. Interleukin-22 ameliorates liver fibrosis through miR-200a/beta-catenin. *Sci Rep.* 2016;6:36436.
 39. Baffy G, Brunt EM, Caldwell SH. Hepatocellular carcinoma in non-alcoholic fatty liver disease: an emerging menace. *J Hepatol.* 2012;56:1384–91.
 40. Rohrig F, Schulze A. The multifaceted roles of fatty acid synthesis in cancer. *Nat Rev Cancer.* 2016;16:732–49.
 41. Xiong X, Zhao Y, Tang F, Wei D, Thomas D, Wang X, et al. Ribosomal protein S27-like is a physiological regulator of p53 that suppresses genomic instability and tumorigenesis. *Elife.* 2014;3:e02236.
 42. Mann J, Chu DC, Maxwell A, Oakley F, Zhu NL, Tsukamoto H, et al. MeCP2 controls an epigenetic pathway that promotes myofibroblast transdifferentiation and fibrosis. *Gastroenterology.* 2010;138:705–714, 714 e701–704.
 43. Moran-Salvador E, Garcia-Macia M, Sivaharan A, Sabater L, Zaki MYW, Oakley F, et al. Fibrogenic activity of MECP2 is regulated by phosphorylation in hepatic stellate cells. *Gastroenterology.* 2019;157:1398–412.e9.
 44. Bian EB, Huang C, Wang H, Chen XX, Tao H, Zhang L, et al. The role of methyl-CpG binding protein 2 in liver fibrosis. *Toxicology.* 2013;309:9–14.
 45. Van Keuren-Jensen KR, Malenica I, Courtright AL, Ghaffari LT, Starr AP, Metpally RP, et al. microRNA changes in liver tissue associated with fibrosis progression in patients with hepatitis C. *Liver Int.* 2016;36:334–43.
 46. Appourchaux K, Dokmak S, Resche-Rigon M, Treton X, Lapalus M, Gattoliat CH, et al. MicroRNA-based diagnostic tools for advanced fibrosis and cirrhosis in patients with chronic hepatitis B and C. *Sci Rep.* 2016;6:34935.
 47. Trebicka J, Anadol E, Elfimova N, Strack I, Roggendorf M, Viazov S, et al. Hepatic and serum levels of miR-122 after chronic HCV-induced fibrosis. *J Hepatol.* 2013;58:234–9.
 48. Miyaaki H, Ichikawa T, Kamo Y, Taura N, Honda T, Shibata H, et al. Significance of serum and hepatic microRNA-122 levels in patients with non-alcoholic fatty liver disease. *Liver Int.* 2014;34:e302–7.
 49. Huang CF, Sun CC, Zhao F, Zhang YD, Li DJ. miR-33a levels in hepatic and serum after chronic HBV-induced fibrosis. *J Gastroenterol.* 2015;50:480–90.
 50. Roderburg C, Mollnow T, Bongaerts B, Elfimova N, Vargas Cardenas D, Berger K, et al. Micro-RNA profiling in human serum reveals compartment-specific roles of miR-571 and miR-652 in liver cirrhosis. *PLoS One.* 2012;7:e32999.

SUPPORTING INFORMATION

Additional supporting information can be found online in the Supporting Information section at the end of this article.

How to cite this article: Chan KK-S, Au K-Y, Fung W-C, Wong C-Y, Chan AC-Y, Lo RC-L. Sex-specific analysis of microRNA profiles in HBV-associated cirrhosis by small RNA-sequencing. *Hepatol Commun.* 2022;6:3473–3486. <https://doi.org/10.1002/hep4.2096>